Vibrational Dynamics of Isotopically Dilute Nitrogen to 104 GPa

H. Olijnyk and A. P. Jephcoat
Department of Earth Sciences, University of Oxford, Oxford OX1 3PR, United Kingdom
(Received 2 July 1998)

Raman studies to 104 GPa of a $^{14}N_2$ host with dilute $^{15}N_2$ and $^{14}N^{15}N$ isotopic species indicate an increase in vibrational coupling with pressure. The lowest frequency branch of the isotopic species $^{15}N_2$ reaches a plateau around 100 GPa suggesting the onset of bond weakening for molecules located on particular sites. An unusual intensity increase is observed for the isotopic ν_1 guest modes. The phase transitions above 20 GPa appear to involve an increase in the number of inequivalent sites, with possibly subtle changes in the orientational behavior of particular molecules in the pressure range 25 to 50 GPa not readily revealed in recent x-ray diffraction studies.

PACS numbers: 62.50.+p, 63.20.–e, 78.30.Hv

The $P - T$-phase diagram of solid nitrogen appears to be well established up to pressures near ~20 GPa [1–10]. At higher pressures the behavior of solid nitrogen is not well understood: Above 25 GPa Raman spectra [8,11] are not compatible with the rhombohedral $R\bar{3}c$ lattice as suggested by x-ray diffraction studies [5–7]; the theoretically predicted tetragonal lattice in this pressure range [12] is in disagreement with experiment; and calculated pressure-volume relations using gas-phase intermolecular potentials for nitrogen [13] significantly depart above 12 GPa from accurate equations of state [6]. A further open question concerns the mechanism responsible for the decrease in frequency of the lower frequency Raman-active vibron above 60 GPa in nitrogen [11,14], that has been discussed in terms of weakening of the N-N bonds under compression as a precursor of molecular dissociation. Indeed theory predicts the molecular to nonmolecular transition well below 100 GPa [15–17], but this is in apparent disagreement with the experimental observation of molecular nitrogen to 180 GPa [11,14] though this discrepancy might be due to the existence of a high-energy barrier associated with molecular dissociation [16,17].

These results demonstrate that we lack a sufficient theoretical description of the interaction potentials and a quantitative understanding of the vibrational dynamics at high pressures. Raman studies of nitrogen isotopic mixtures have provided a measure of the intermolecular and intramolecular interactions, but have been limited to moderate pressures [8]. We report Raman measurements at room temperature up to 104 GPa for the internal modes of $^{14}N_2$ as host, and for the isotopic species $^{15}N_2$ and $^{14}N^{15}N$ as dilute (guest) molecules. Shifts and splittings of the internal modes in the solid state result from the local anisotropy of the crystalline field (site-group interactions) as well as from the coupling of identical vibrations of adjacent molecules in the unit cell (variously known as factor-group interactions, and dynamic, vibrational, or resonance coupling). At low concentrations, the isotopically substituted molecules are isolated in the host matrix and the coupling effect is switched off for these guest isotopic species because of the frequency difference with the corresponding vibrations of the host ($^{14}N_2$) [2]. The difference between the frequency of the isotopically substituted molecule and the frequency of the same mode in the host crystal, if corrected for the different masses, provides a measure of the intermolecular coupling constant. In addition, splittings due to nonequivalent sites can be distinguished from factor-group splittings and can give valuable insight into changes in the crystal structure.

We diluted pure $^{15}N_2$ in $^{14}N_2$ up to nominal concentrations of 3% and 0.7% $^{15}N_2$. After waiting several days to allow for mixing, the samples were loaded into a diamond-anvil cell at 0.2 GPa with a gas-loading technique. The concentrations estimated from the ν_2 intensity ratios are 3% and 0.5% for $^{15}N_2$ in approximate agreement with the nominal concentrations in the original mixture. For the naturally abundant $^{14}N^{15}N$ molecule, this method gave 1.4% and 0.7%, respectively. The signal-to-background ratio of the weak signals from the isotopic species was improved by selecting ultralow fluorescence diamonds and excitation with the 647.1-nm line of a Kr^+ laser to reduce diamond fluorescence. Scattered light was collected through a spatial filtering aperture and analyzed at an angle of 135° with respect to the incoming laser beam using a 0.6-m triple spectrograph and a liquid nitrogen cooled charge-coupled device multichannel detector. Pressure was determined with the quasihydrostatic ruby fluorescence scale. In the probed central sample region of ~15 μm in diameter, the pressure differences were about 1 GPa at the maximum pressure of the study. Both ruby lines were clearly resolved up to the maximum pressure; the R_1-R_2 line splitting and the R_1 half-width had values similar to those observed in solid N_2 between 20 and 37 GPa by Le Sar *et al.* [1] indicating that the pressure inhomogeneities in the present study were low.

For the $R\bar{3}c$ lattice the stretching mode is divided into two main branches ν_1 and ν_2 as required by the two different $2b$ and $6e$ sites. For the ν_2 branch, two Raman-active peaks due to factor-group splitting, A_{1g} and E_g, are to be expected [3]. Raman spectra of the internal modes

 0031-9007/99/83(2)/332(4)$15.00

of the $^{14}N_2$ host at different pressures are shown in Fig. 1, and the pressure shift of the mode frequencies in Fig. 2. Between 16 GPa and ~30 GPa, the number of observed internal modes is consistent with a $R\bar{3}c$ lattice. A third branch in the ν_2 frequency region, ν_{2a}, is observed above 30 GPa (Fig. 2). In the ν_{2c} branch a second component ($\nu_{2c(2c)}$) appears on the low-frequency side around 40 GPa, which corresponds to the peak assigned as $\nu_{2c(3)}$ in the study of Schneider *et al.* [8]. A third component $\nu_{2c(2b)}$ (not previously documented) appears at 65 GPa, and can be related to the phase transition documented at this pressure by clear changes in the x-ray diffraction pattern [5], as well as the appearance of $\nu_{2c(1b)}$. In contrast to previous reports [11,14] we observe three modes instead of one mode above 65 GPa in the $\nu_{2c(2)}$ branch in $^{14}N_2$ which exhibit a broad maximum around 75 GPa in their frequency-pressure curves. We note that Raman spectra (unpublished) of the study of Reichlin *et al.* [11] clearly show evidence from shoulders and asymmetries that their $\nu_{2c} \rightarrow \nu_{2c(2)}$ band is composed of more than one mode above 40 GPa. Because all the other modes have much smaller half-widths above 40 GPa than the $\nu_{2c} \rightarrow \nu_{2c(2)}$ band, pressure inhomogeneities can be ruled out as an explanation for the effect; furthermore, the spectrum at 68 GPa shown in Fig. 1, which was taken after the sample was melted by laser heating to reduce nonhydrostatic stress, did not result in a decrease of the ν_{2c} half-width, but clearly shows the triplet structure of the $\nu_{2c(2)}$ band as judged by the presence of low- and high-frequency shoulders. Mode $\nu_{2c(1a)}$, which was taken as an indicator for a further phase transition at 100 GPa in the previous study [11], is already observed around 85 GPa in the present study. Modes ν_{2a} and ν_1, which were lost in the background in the previous experiment [11] between 60 and 80 GPa, could be observed to the maximum pressure in the present experiments, but with much reduced intensity. The persistence of the lower-pressure modes at the highest pressures indicates a close structural relationship among the various high-pressure phases.

The isotopic modes of $^{15}N_2$ were observed up to 104 GPa and overlap with $^{14}N^{15}N$ modes occurred above 80 GPa. The vibrons of the $^{14}N^{15}N$ molecule were followed to 40–50 GPa, where they began to merge with the $^{14}N_2$ host vibrons. The inequivalence of the nitrogen isotopes in the $^{14}N^{15}N$ molecule introduces a small permanent electric dipole moment and head-to-tail disorder. The associated changes in the interactions with the surroundings must be very small because there was no noticeable difference in the behavior of the $^{15}N_2$ and the $^{14}N^{15}N$ modes. We did not observe any difference in the spectral features and their pressure dependence between the two different concentrations. Raman spectra of the guest isotopic species are shown in Fig. 1. Starting at 11 GPa, for both isotopic species, two modes, ν_1 and ν_2, are observed as expected. Above 25 GPa, ν_2 becomes asymmetric and increasingly broader. Since ν_1 remains narrow, nonhydrostatic stress effects can also be ruled out as a reason for this broadening—rather the result suggests a splitting into two components. These observations therefore indicate that in this pressure range the guest ν_2 modes arise from

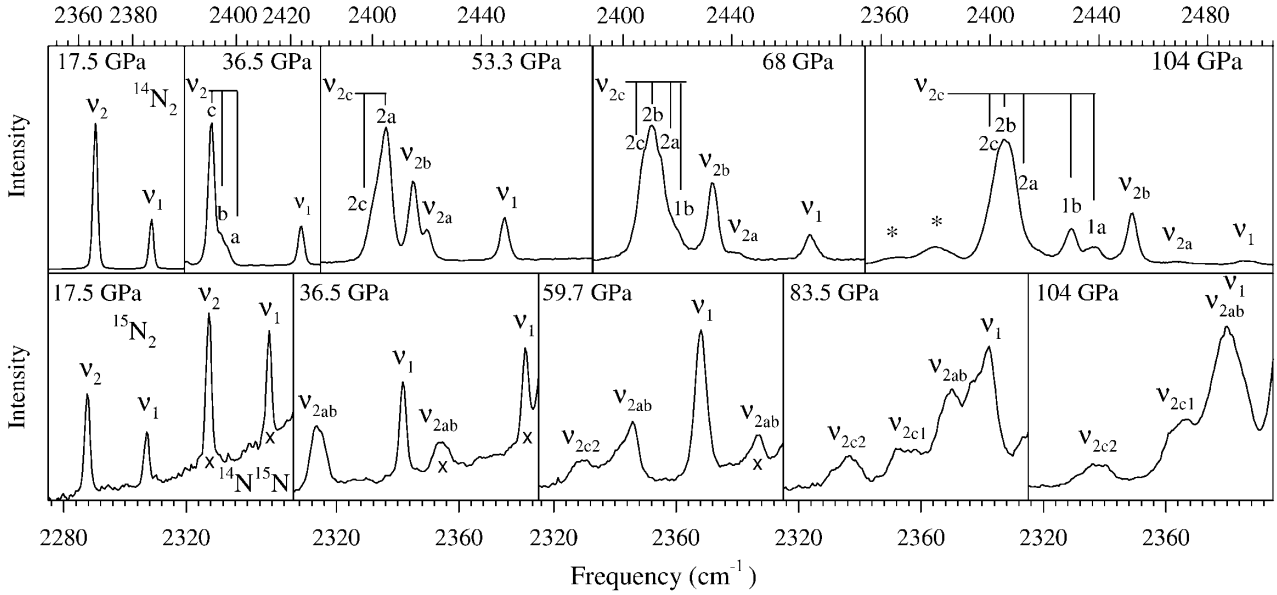

FIG. 1. Upper panel: Raman spectra of the internal modes of $^{14}N_2$ at various pressures. The spectrum at 17.5 GPa is from the 0.5% $^{15}N_2$ enriched sample, the spectrum at 68 GPa from a nonenriched $^{14}N_2$ sample, which was melted by heating with a Nd:YAG laser using a ruby chip as an absorber to reduce nonhydrostatic stress. Remaining spectra are from the 3% $^{15}N_2$ enriched sample. Isotopic species are marked with ∗. Lower panel: Raman spectra of internal modes of $^{14}N^{15}N$ and $^{15}N_2$ isotopic species at various pressures. The spectrum at 17.5 GPa is from the 0.5% $^{15}N_2$ enriched sample, whereas the remaining spectra are from the 3% $^{15}N_2$ enriched sample. $^{14}N^{15}N$ modes are marked with a cross.

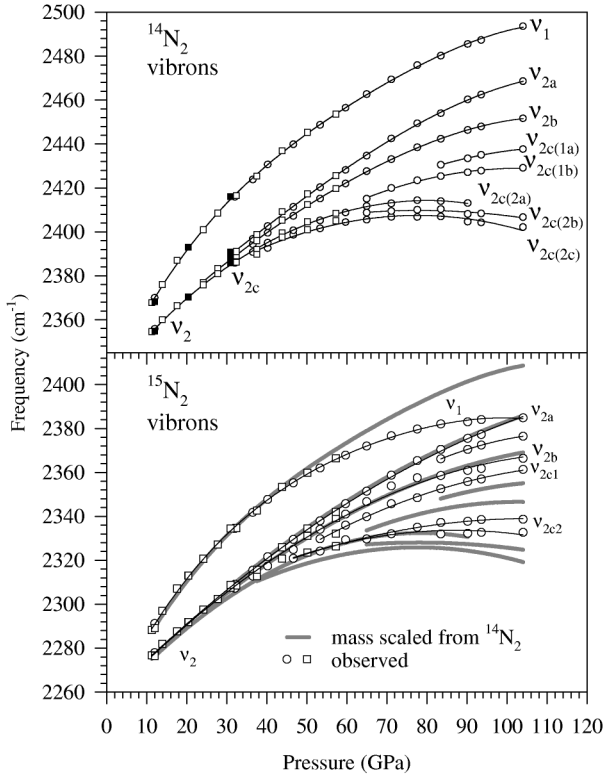

FIG. 2. Upper panel: Pressure shift of Raman-active $^{14}N_2$ vibrons. Circles: sample with 3% $^{15}N_2$; squares: sample with 0.5% $^{15}N_2$; open symbols: pressure increase; solid symbols: pressure decrease. The solid lines serve as a guide for the eye. Lower panel: Pressure dependence of Raman-active internal modes of $^{15}N_2$ isotopic species. The circles and squares refer to the 3% and 0.5% enriched $^{15}N_2$ samples, respectively. The thin solid lines are guides for the eye. Thick grey lines show the expected pressure shift of the isotopic modes due to changes in mass as calculated by $\nu_{\rm iso} = \nu_{\rm host}\sqrt{(\mu_{\rm host}/\mu_{\rm iso})}$, where μ is the reduced mass.

molecules located on two inequivalent sites, in disagreement with an ordered $R\bar{3}c$ lattice for which only one site gives rise to the ν_2 modes. A triplet structure is observed in ν_2 of the $^{14}N_2$ host between 30 and 40 GPa (Fig. 1) and implies one of the isotopic ν_2 modes is doubly degenerate and one splitting in the $^{14}N_2$ host, probably ν_{2c} (because the two isotopic modes track the curves given by ν_{2a} and ν_{2b} of the host, see Fig. 2), is due to factor-group interactions. The fact that x-ray diffraction studies [5–7] show no phase transition in this pressure range indicates that subtle structural changes probably in the orientational behavior of molecules located on the 6*e* site take place, resulting in two sites with slightly different symmetry. Additional modes appear in the isotopic ν_2 region above 47 GPa. The spectral features are not well resolved in this pressure regime but at the highest pressures one can distinguish at least three branches in the ν_2 frequency region of $^{15}N_2$. Asymmetries may indicate that these branches involve more than one component at the highest pressures. The branchings observed for the isotopic modes are observed at approximately the same pressures as in the $^{14}N_2$ host and indicate that the associated structural changes are accompanied by an increase in the number of inequivalent sites.

The pressure shifts of the isotopic species mode frequencies are also compared to the mass-scaled frequencies of the $^{14}N_2$ host in Fig. 2. With the exception of ν_{2a} and probably ν_{2b}, the guest modes deviate from the curves expected from the mass-scaled host modes. The ν_{2c2} modes show a positive frequency shift relative to the $^{14}N_2$ host. The ν_1 guest modes also show a slight positive frequency shift below 30 GPa, but at higher pressures the shift becomes increasingly negative, as plotted in Fig. 3 that shows the ν_1 guest-host frequency ratio of both dilute isotopic species. Theoretical estimates have shown that the magnitude of vibrational coupling depends on the orientation of the molecules as well as on the distance between them [10]. With regard to the softening of the guest ν_1, we note that the ν_1 of the van der Waals compound $He(^{14}N_2)_{11}$ shows a similar negative frequency shift relative to pure $^{14}N_2$ above 30 GPa [18] and can be interpreted in terms of interference by He in the host intermolecular interaction [19]. For the ν_1 mode, significant changes in the intensity with pressure are involved and are also shown in Fig. 3 where the ν_1 guest-host intensity ratio increases approximately exponentially with pressure. The ν_1 intensity of the 3% $^{15}N_2$ is comparable to that of the host ν_1 at the maximum pressure, despite its low concentration. Extrapolation of the trend to normal pressure, below the first data point of this study at ~10 GPa, agrees approximately with the effective guest species concentrations and suggests that the perturbation on the intensity is already under way at low pressures.

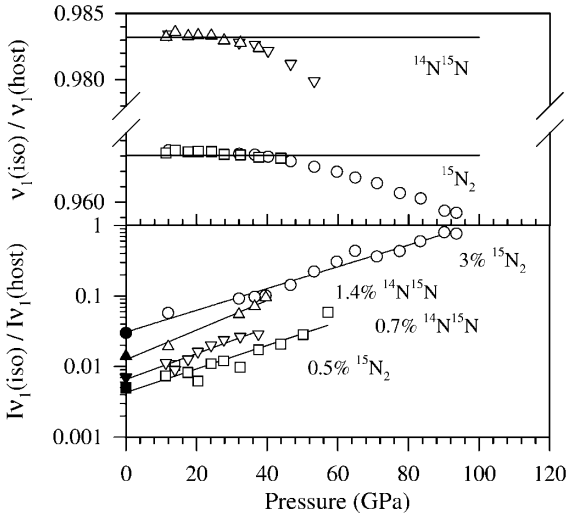

FIG. 3. Upper panel: Guest-host frequency ratio for the ν_1 modes as a function of pressure. The horizontal lines represent the square root of the reduced mass ratio. Lower panel: Pressure dependence of the guest-host ν_1 intensity ratios for the various concentrations. The solid symbols at ambient pressure are the estimated concentrations. The solid lines serve as guides for the eye.

The reasons for these intensity perturbations observed for the ν_1 guest modes are unclear at present.

A clear result of this study is that the lowest frequency mode of the ν_2 branch of the guest molecules, visible above 50 GPa, shows behavior similar to the corresponding host mode, but with a delayed turnover in frequency to above 100 GPa. On the other hand, the ν_1 guest mode reaches a plateau at 104 GPa (i.e., lower in pressure than expected for the $^{14}N_2$ host) even though diluted and not subject to vibrational coupling. With vibrational coupling negligible for the dilute isotopic species, a turnover in the vibron frequency may be related to the onset of bond weakening (as was suggested in the case of solid H_2 from the turnover of the infrared vibron [20], also not subject to vibrational coupling), but for molecules located on particular sites only, as not all branches show negative frequency shift with pressure. A possible scenario emerging from the present results might be that molecular dissociation in nitrogen starts in molecules at particular sites lending some support to the hypothesis of the formation of conducting chains or clusters associated with the transition into the metallic state, as discussed for nitrogen by Schiferl *et al.* [2] and for hydrogen by Hohl *et al.* [21].

The dependence of vibrational coupling in molecular solids on the density and, in particular, details of the crystal structure could be far more complex than previously thought. The results here support the presence of increased vibrational coupling under pressure for the $\nu_{2c(2)}$ host modes, but the early turnover of the ν_1 *guest* vibron cannot be attributed to vibrational coupling because this interaction should be switched off in the present experiment. Reconciliation of these results may require a difference in the *sign* of the vibrational coupling interaction at particular sites in the host. Furthermore, compression also results in a significant (unexplained) intensity enhancement of the ν_1 guest vibrons. The situation is made more complex through the recent result that the turnover of the Raman and infrared vibron in solid H_2 need not require charge transfer or the onset of bond weakening [22]. Finally, the isotopic spectra are shown to be of great importance for the identification of different site symmetries not easily detected in x-ray diffraction. This may have significant implications for future attempts at the resolution of structures from powder x-ray diffraction, for example in the high-pressure phases of the solid hydrogens [23], which also display complex rotational and vibrational effects [20]. The present data provide important constraints on structures in the 100-GPa regime and suggest new theoretical effort will be essential for a quantitative interpretation of highly condensed solid nitrogen.

We acknowledge support from the European Union under Contract No. GE1*CT92-0046 that made possible preliminary studies at the European Laboratory for Non-Linear Spectroscopy (LENS).

[1] R. LeSar, S. A. Ekberg, L. H. Jones, R. L. Mills, L. A. Schwalbe, and D. Schiferl, Solid State Commun. **32**, 131 (1979).
[2] D. Schiferl, R. LeSar, and D. S. Moore, in *Simple Molecular Systems at Very High Density*, edited by A. Polian, P. Loubeyre, and N. Boccara (Plenum Press, New York, 1989), p. 303, and references therein.
[3] D. Schiferl, S. Buchsbaum, and R. L. Mills, J. Phys. Chem. **89**, 2324 (1985).
[4] R. L. Mills, B. Olinger, and D. T. Cromer, J. Chem. Phys. **84**, 2837 (1986).
[5] A. P. Jephcoat, R. J. Hemley, H. K. Mao, and D. E. Cox, Bull. Am. Phys. Soc. **33**, 522 (1988).
[6] H. Olijnyk, J. Chem. Phys. **93**, 8968 (1990).
[7] M. Hanfland, M. Lorenzen, C. Wassilew-Reul, and F. Zontone, in *Proceedings of the International Conference on High Pressure Science and Technology, Kyoto, Japan* [Rev. High Pressure Sci. Technol. **7**, 787 (1998)].
[8] H. Schneider, W. Häfner, A. Wokaun, and H. Olijnyk, J. Chem. Phys. **96**, 8046 (1992).
[9] M. I. M. Scheerboom and J. A. Schouten, Phys. Rev. Lett. **71**, 2252 (1993).
[10] M. I. M. Scheerboom and J. A. Schouten, J. Chem. Phys. **105**, 2553 (1996).
[11] R. Reichlin, D. Schiferl, S. Martin, C. Vanderborgh, and R. L. Mills, Phys. Rev. Lett. **55**, 1464 (1985).
[12] J. Belak, R. LeSar, and R. D. Etters, J. Chem. Phys. **92**, 5430 (1990).
[13] R. D. Etters, V. Chandrasekharan, E. Uzan, and K. Kobashi, Phys. Rev. B **33**, 8615 (1986).
[14] P. M. Bell, H. K. Mao, and R. J. Hemley, Physica (Amsterdam) **139B&140B**, 16 (1986).
[15] A. K. McMahan and R. LeSar, Phys. Rev. Lett. **54**, 1929 (1985).
[16] R. M. Martin and R. J. Needs, Phys. Rev. B **34**, 5082 (1986).
[17] C. Mailhiot, L. H. Yang, and A. K. McMahan, Phys. Rev. B **46**, 14 419 (1992).
[18] H. Olijnyk and A. P. Jephcoat, J. Phys. Condens. Matter **9**, 11 219 (1997).
[19] M. I. M. Scheerboom, J. P. J. Michels, and J. A. Schouten, J. Chem. Phys. **104**, 9388 (1996).
[20] H. K. Mao and R. J. Hemley, Rev. Mod. Phys. **66**, 671 (1994).
[21] D. Hohl, V. Natoli, D. M. Ceperley, and R. M. Martin, Phys. Rev. Lett. **71**, 541 (1993).
[22] M. I. M. Scheerboom and J. A. Schouten, Phys. Rev. B **53**, 14 705 (1996).
[23] S. P. Besedin, A. P. Jephcoat, M. Hanfland, and D. Häusermann, Appl. Phys. Lett. **71**, 470 (1997).